Journal of Cellular Physiology

Grb10 Deletion Enhances Muscle Cell Proliferation, Differentiation and GLUT4 Plasma Membrane Translocation

NANCY MOKBEL,[1]* NOLAN J. HOFFMAN,[1] CHRISTIAN M. GIRGIS,[2,3] LEWIN SMALL,[1] NIGEL TURNER,[4] ROGER J. DALY,[5] GREGORY J. COONEY,[1]* AND LOWENNA J. HOLT[1]

[1] *Diabetes and Obesity Research Program, The Garvan Institute of Medical Research, Sydney, New South Wales, Australia*

[2] *Immunology-Diabetes and Transcription Research Program, The Garvan Institute of Medical Research, Sydney, New South Wales, Australia*

[3] *Faculty of Medicine, The University of Sydney, Sydney, New South Wales, Australia*

[4] *Department of Pharmacology, School of Medical Sciences, University of New South Wales, Sydney, New South Wales, Australia*

[5] *Department of Biochemistry and Molecular Biology, Monash University, Melbourne, Victoria, Australia*

Grb10 is an intracellular adaptor protein which binds directly to several growth factor receptors, including those for insulin and insulin-like growth factor receptor-1 (IGF-1), and negatively regulates their actions. Grb10-ablated ($Grb10^{-/-}$) mice exhibit improved whole body glucose homeostasis and an increase in muscle mass associated specifically with an increase in myofiber number. This suggests that Grb10 may act as a negative regulator of myogenesis. In this study, we investigated in vitro, the molecular mechanisms underlying the increase in muscle mass and the improved glucose metabolism. Primary muscle cells isolated from $Grb10^{-/-}$ mice exhibited increased rates of proliferation and differentiation compared to primary cells isolated from wild-type mice. The improved proliferation capacity was associated with an enhanced phosphorylation of Akt and ERK in the basal state and changes in the expression of key cell cycle progression markers involved in regulating transition of cells from the G1 to S phase (e.g., retinoblastoma (Rb) and p21). The absence of Grb10 also promoted a faster transition to a myogenin positive, differentiated state. Glucose uptake was higher in $Grb10^{-/-}$ primary myotubes in the basal state and was associated with enhanced insulin signaling and an increase in GLUT4 translocation to the plasma membrane. These data demonstrate an important role for Grb10 as a link between muscle growth and metabolism with therapeutic implications for diseases, such as muscle wasting and type 2 diabetes.

J. Cell. Physiol. 229: 1753–1764, 2014. © 2014 Wiley Periodicals, Inc.

Skeletal muscle is a highly dynamic tissue that makes up 25%–40% of our body weight (Janssen et al., 2000). It is capable of increasing in size and improving in function after various physiological stimuli (e.g., exercise, weight bearing), and injuries. Muscle is also a major tissue contributing to energy balance, and can be responsible for up to 80% of insulin-stimulated glucose uptake and storage after a meal (DeFronzo et al., 1985; Shulman et al., 1990). Change in muscle mass is one of the factors shown to significantly affect glucose homeostasis and metabolic health. An increase in muscle mass after exercise training is associated with overall improved glucose utilization and reduced insulin resistance (Srikanthan and Karlamangla, 2011). Conversely, reduced muscle bulk during aging and severe myopathic diseases is associated with insulin resistance, a risk factor for type 2 diabetes (Evans, 1997; Cruz Guzman Odel et al., 2012). Thus, identifying factors or mechanisms that regulate muscle growth, regeneration, and metabolism could provide therapeutic targets to improve metabolic health, and has implications for treatment of muscle diseases, and maintaining general muscle function during aging.

The regenerative capacity of muscle is attributed to the activation of a specialized population of cells termed "satellite cells" that reside between the basal lamina and sarcolemma of muscle fibers. Muscle satellite cells share the same origin as embryonic muscle precursor cells (Gros et al., 2005) and act as adult stem cells in skeletal muscle. Therefore, they are considered the major contributors to skeletal muscle growth and regeneration in adults. Under normal conditions, satellite cells are in a quiescent state (G_0 phase), and in response to trauma, injury, or stress, they become activated and enter mitosis to proliferate then exit the cell cycle to differentiate and form new fibers (hyperplasia) or fuse to existing myofibers (hypertrophy) (Hawke and Garry, 2001). The main growth factors that have been shown to regulate satellite cell proliferation and differentiation include IGF-1 & IGF-2 (Duclos et al., 1991; McFarland et al., 1993), the fibroblast growth factor (FGF) family (Bendall et al., 2007), hepatocyte growth factor (HGF) (Maina et al., 1996; Tatsumi et al., 1998), and transforming growth factor (TGF)-beta (Bischoff, 1990;

Conflict of interest: none.

Contract grant sponsor: National Health and Medical Research Council (NHMRC) of Australia;
Contract grant number: 481335.

*Correspondence to: Nancy Mokbel & Gregory J. Cooney, Diabetes and Obesity Program, The Garvan Institute of Medical Research, Darlinghurst, New South Wales, 2010, Australia.
E-mail: n.mokbel@garvan.org.au or nmok1@hotmail.com, g.cooney@garvan.org.au

Manuscript Received: 1 December 2013
Manuscript Accepted: 21 March 2014

Accepted manuscript online in Wiley Online Library (wileyonlinelibrary.com): 24 March 2014.
DOI: 10.1002/jcp.24628

Yablonka-Reuveni and Rivera, 1997). These growth factors trigger a cascade of downstream signaling that phosphorylate myogenic regulatory factors (MRF) leading to the regulation of proliferation and/or differentiation of satellite cells (Yablonka-Reuveni and Rivera, 1994; Sabourin and Rudnicki, 2000; Le Grand and Rudnicki, 2007).

The Grb10 gene encodes for a growth factor receptor-binding protein that is abundantly expressed in major insulin-sensitive tissues such as muscle and adipose tissue, as well as pancreas (Smith et al., 2007; Wang et al., 2007). Grb10 binds, and negatively regulates signal output from the insulin receptor (IR) (Liu and Roth, 1995; O'Neill et al., 1996; Laviola et al., 1997; Ramos et al., 2006), and IGF-1 receptor (IGF-1R) (Liu and Roth, 1995; Morrione et al., 1996; Laviola et al., 1997). Grb10 also interacts in vitro with other growth factor receptors such as those for epidermal growth factor (EGF) (Ooi et al., 1995), platelet-derived growth factor (PDGF), fibroblast growth factor (FGF), and HGF receptors (Wang et al., 1999; Holt and Siddle, 2005; Liu et al., 2012), but the physiological relevance of Grb10 binding in this context is unclear. Studies from our laboratory and others have demonstrated that deletion of Grb10 in mice results in improved glucose metabolism mediated by enhanced insulin signaling and increased phosphorylation of insulin receptor substrate-1 (IRS1) in muscle (Smith et al., 2007; Wang et al., 2007; Holt et al., 2009). More recently, we have identified a novel role for Grb10 in regulating muscle mass (Holt et al., 2012). Mice lacking Grb10 have significantly elevated muscle mass compared to wild-type (WT). This is mainly due to hyperplasia, with no change in fiber size or proportion. This model of hyper-muscularity is unlike other models such as IGF-1 transgenic mice (Coleman et al., 1995; Musaro et al., 2001) and myostatin knock-out mice (McPherron et al., 1997), which exhibit both hyperplasia and hypertrophy.

The knowledge of the role of Grb10 in muscle outside of insulin signaling pathway regulation is limited. The aim of the current study was to understand the mechanisms underlying the increase in muscle mass and glucose homeostasis in the $Grb10^{-/-}$mice. Thus, we investigated the impact of Grb10 deletion on muscle cell proliferation, differentiation, and glucose metabolism in an in vitro model of pure primary muscle cells isolated from WT and $Grb10^{-/-}$ mice. The results supported a role for Grb10 in playing a regulatory link between muscle growth and metabolism.

Materials and Methods

Animal maintenance

Mice with homozygous deletion of Grb10 ($Grb10^{-/-}$) have been described previously in (Charalambous et al., 2003) and were maintained on a mixed C57BL/6 x CBA background at the Australian Bioresources (ABR) as described in Holt et al., 2012. All animal studies were performed with the approval of the Garvan Institute/St Vincent's Hospital Animal Ethics Committee.

In vitro isolation and maintenance of mouse-derived primary muscle cells

Mouse primary myoblast cell lines were established from WT and $Grb10^{-/-}$ mice using explant culture (Decary et al., 1997) with some modifications as outlined below. Quadriceps muscles from four-week-old mice were dissected out and rinsed in PBS containing 40 μg/ml gentamicin. Muscle was cleaned from surrounding tissue, fat, and vasculature, and then transferred into ~0.5–1.0 ml of plating media (DMEM/HAMS-F12 media 1:1, 40% v/v heat-inactivated FBS (Thermo Fisher Scientific), 10% v/v amniomax, 40 μg/ml gentamicin). The muscle was then cut into 1 mm^3 pieces and placed as explants in culture dishes (Becton Dickinson) coated with collagen–matrigel (DMEM/HAMS-F12 1:1. 0.17 mg/ml collagen type I (Becton Dickinson), 1/50 dilution of matrigel (Becton Dickinson), 40 μg/ml gentamicin). Dishes were kept in a humidified chamber at 37 °C, 5% CO_2 and after 48 h, when the explants had sufficiently adhered, 2 ml of myoblast media (DMEM/HAMS-F12 1:1, 10% v/v amniomax, 20% v/v FBS, 40 μg/ml gentamicin) was added. Once outgrowth from the explants was visible (day 2 or 3), cells were gently washed twice with 1xPBS and detached using TrypLE. The cells were then transferred and expanded in a T75 flask. At 60%–70% confluency, expanded cells were detached with TrypLE and centrifuged at 300 g for 15 min. Media was then aspirated and the pellet frozen down in myoblast media + 10% DMSO. For differentiation of primary myoblasts into myotubes, myoblast media was replaced with a differentiation media (DM) (DMEM/HAMS-F12 1:1 media (12.5 nM glucose), antibiotics, 40 μg/ml gentamicin, 3% heat-inactivated horse serum). Cells were allowed to differentiate into mature myotubes over 6 days. For all assays, a total of six clones from WT and $Grb10^{-/-}$ mice was used, and clones were maintained in the same culture media conditions with similar passage number.

Purification of satellite cells by FACS

Enrichment of primary muscle cells was achieved by FACS using a Neural Adhesion Cell Marker/CD56 (NCAM/CD56) antibody (MEM-188, Thermo Scientific/Pierce). Isolated primary cells were left in culture for 48 h before sorting in order to enhance the expression of cell surface markers. Cells were centrifuged at 300 g for 1 min, then the pellet washed with 1 ml of FACS buffer (1 x sterile PBS + 0.1% BSA). The cell suspension was centrifuged at 300 g for 1 min, and the pellet suspended in 100 μl FACS buffer containing NCAM/CD56 antibody, 1:10. Cells were incubated on ice for 20 min and were washed twice in FACS buffer in preparation for sorting. Cell sorting was performed using a FACS Aria U2 (Becton Dickinson) at 4 °C with a 100 μm nozzle. To eliminate false positive cells, the preparation was sorted against auto fluorescence parameters with a 530 nm filter. For all WT and $Grb10^{-/-}$ clones included in this study, the top 20th percentile of the NCAM/CD56 positive cells was collected containing the most intensely staining NCAM/CD56 positive cells. All satellite cells were used at low passage (1–9).

RNA isolation, cDNA synthesis and real time qPCR

Total RNA isolation from mouse tissues, primary cultured myoblasts and myotubes was performed using the TRIZOL Reagent® method (Sigma-Aldrich, Castle Hill, Australia) as per the manufacturer's instructions, followed by ethanol precipitation. cDNA was synthesized from 1 μg of total RNA using the Omniscript RT Kit (200) (Qiagen, VIC, Australia) and Random Primer 9 (New England Biolabs, MA). The intron-spanning primer set used were as follows: for mouse Grb10 (UPL probe#63), forward 5′-CGGTTGCTCCTAGCTCCTT-3′, reverse 5′-CTGAAGCCTGGAGGGAAAT-3′, for mouse cyclophillin (UPL probe# 108), forward 5′-ATCTGCTCGCAATACCCTGT-3′, reverse 5′-CTTGAAGGGGAATGAGGAAA, for mouse p21 (SYBR Green), forward 5′-GCCTTAGCCCTCACTCTGTG-3′, reverse 5′-AGGGCCCTACCGTCCTACTA-3′. Data analysis was performed using the comparative 2-delta Ct method and normalized tocyclophilin transcript.

Immunohistochemical analysis

Cells grown on collagen/Matrigel coated plastic Thermanox coverslips (Nunc, Rochester, NY) were fixed and permeabilized in 3% PFA/0.1% Triton-X 100/PBS. Immunocytochemistry was performed as previously described (Ilkovski et al., 2004). Imaging was undertaken using a Zeiss AxioPlan1 upright microscope and a Nikon Super Resolution Microscope N-SIM. Primary antibodies used for immunohistochemical analysis were incubated overnight

at 4 °C and included: PAX7 (1:50, Hybridoma Bank, UIOWA) and MyoD (1:100, Santa Cruz). Antibodies incubated at room temperature for 3 h included: sarcomeric actin (5C5 1:500, Sigma-Aldrich), α-actinin 2 (4B3, 1:500,000, kindly provided by Prof. Kathryn North, Institute of Neuroscience and Muscle Research, Westmead, Australia) and total myosin heavy chain (MF 30,1:500, Hybridoma Bank, UIOWA).

Immuno-blotting

Protein lysates were collected from primary myoblasts at day 2 (D2), myotubes at day 6 of differentiation (Diff 6) and muscle tissue isolated from WT and Grb10$^{-/-}$ mice. Samples from cells and tissue were solubilized in a lysis buffer containing (4% SDS, 62.5 mM TrispH 6.8, 10% glycerol, 1:500 protease inhibitors cocktail). Lysates collected from cells were left on ice for ~15 min then sonicated to shear chromosomal DNA. Muscle samples collected from WT and Grb10$^{-/-}$ mice were processed as described in (Hoy et al., 2007). Primary antibodies used for immunoblotting included: Grb10 antibody (K20, 1:1000, Santa Cruz), total retinoblastoma (t-Rb) (1:1000, BD Pharmingen), phospho-retinoblastoma S807 (p-Rb) (1:1000,CST), total Akt (t-Akt) and phospho-Akt S473 (p-Akt) (1:1000, CST), total ERK (t-ERK) and phospho-p44/42 MAPK (Erk1/2) (Thr202/Tyr204) (p-ERK) (1:1000, CST), skeletal actin 5C5 (1:2000, Sigma-Aldrich), vimentin (1:1000, Sigma-Aldrich), myogenin (F5D, 1:1000, Hybridoma Bank, UIOWA), β-tubulin (E7,1:1000, Hybridoma Bank, UIOWA).

In vitro proliferation assay

Cell proliferation rate was measured by a BrdU ELISA (Roche, USA). Briefly, satellite cells were seeded at ~6000 cells/cm^2 on collagen–matrigel coated 96 well plates and pulsed with 10 μM of BrdU 2 h after seeding (T0) and incubated for 4 h. BrdU antibody was used at 1:100 and fluorescence was read at 570 nm using a fluorescent microtiter plate reader (Fluostar Omega-BMG Labtech, Ortenberg, Germany). For the manual cell count, cells were seeded at low density at ~200 cells/cm^2 and counted using a haemocytometer at 24 h intervals.

Growth factor studies

Primary myoblasts and myotubes were serum starved for 4 h and 6 h respectively (baseline) followed by growth factor stimulation with insulin (6 min), IGF-1 (6 min) and HGF (20 min), and protein lysates collected. Growth factors were used at concentrations: insulin (100 nM, Actrapid Penfill, 100 IU units/ml), IGF-1 (10 ng/ml, EAG-c03, Gropep, Adelaide, Australia), HGF (50 ng/ml, 130-093-872, Miltenyi Biotech, Macquarie Park, Australia). These concentrations were determined as optimal concentrations for activation of Akt and ERK.

Glucose uptake assay

To assess the rate of glucose uptake in cells, differentiated primary myotubes-Diff 6 were serum starved for 6 h in a media containing DMEM/HAMS-F12 (6 mM glucose). The assay was performed as described in (Tan et al., 2010) with minor modifications outlined below. Briefly, cells were stimulated with insulin (100 nM) for 15 min in Krebs buffer and for the final 5 min of stimulation 0.2 mM of 2-deoxyglucose (D3179-1G, Sigma-Aldrich) + 10 μCi/ml 1,2-^{3}H radioactively labelled 2-deoxyglucose (2DG, Perkin Elmer, Massachusetts) was added to assess glucose uptake. After 5 min 2DG stock was removed and lysis buffer (2% SDS, 125 mM Tris-HCl pH 6.8) was added. Specific activity (dpm ^{3}H/pmole) of glucose was read using a Beta counter (Beckman LS 6500) and results were normalized to total protein content.

GLUT4 translocation assay

GLUT4 translocation assay was performed as described in (Govers et al., 2004), (Shewan et al., 2003) with minor modifications outlined below. Satellite cells were transduced with HA-GLUT4 retrovirus and measurement of cell surface

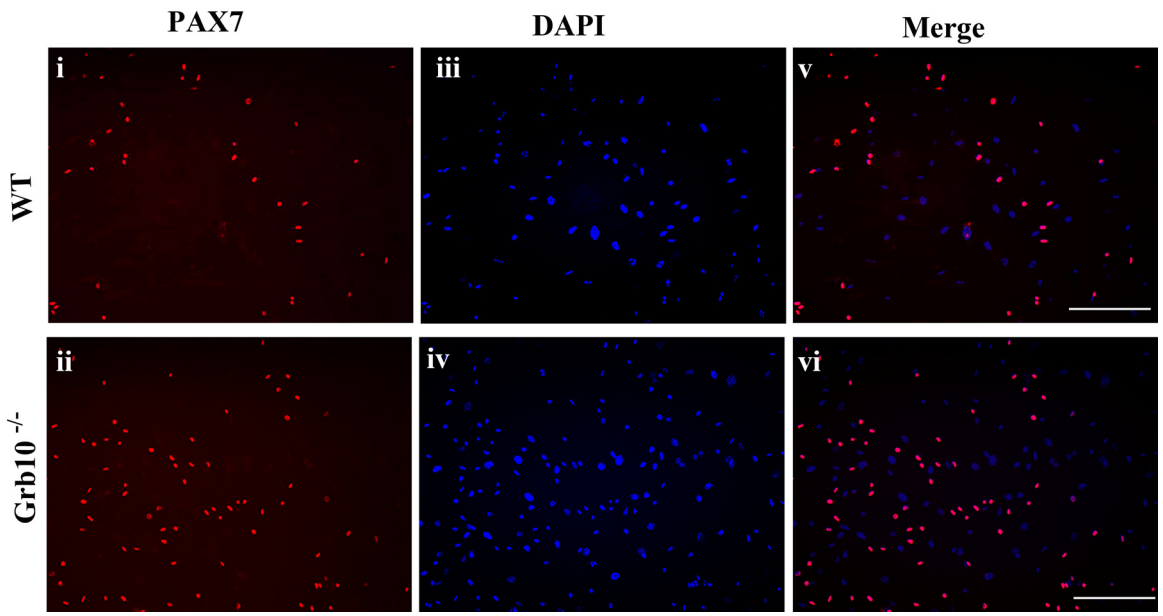

Fig. 1. Assessment of satellite cell content in primary muscle cultures prior to purification with NCAM/CD56 antibody. (i&ii) Representative images from WT and Grb10$^{-/-}$ primary muscle cells respectively showing ~20 and 40% of PAX7 positive cells compared to (iii&iv) the total number of cells (shown by DAPI stain). The merged images (v&vi) show co-localisation of PAX7 positive cells (red) with total number of cells (blue). Images were taken on a Zeiss Axioplan microscope with a 10x objective. Scale bar 50 μm.

HA-GLUT4 as a percentage of total cellular HA-GLUT4 was performed. Differentiated myotubes were serum-starved for 4 h in 1:1 DMEM/HAMS-F12, and maintained in this medium during subsequent treatments. Myotubes were stimulated with 100 nM insulin for the final 20 min of serum starvation. All values were expressed as a percentage of total GLUT4 that was determined from anti-HA antibody labeling of permeabilized cells.

Statistical analysis

All data presented are expressed as means ± SEM where appropriate. Statistical analysis was performed by two-way analysis of variance (ANOVA) where appropriate using GraphPad Prism Version 6. Unpaired *t*-tests, two tailed distribution, and unequal variance were applied. Statistical significance was set a priori at $P \leq 0.05$.

Results

Isolation and characterization of a highly myogenic NCAM/CD56+ subpopulation of cells from mouse skeletal muscle

Primary cells isolated from muscle of four-week-old WT and Grb10$^{-/-}$ mice represent a highly enriched, but mixed, myogenic cell population. Using PAX7, as a marker of satellite cells, we demonstrated that ~20% and 40% respectively of WT and Grb10$^{-/-}$ cells isolated are satellite cells (Fig. 1). To further enrich for primary muscle cells, cells from these cultures were sorted using FACS based on the expression of the neural cell adhesion marker NCAM/CD56 previously described to be expressed on muscle progenitor cells derived from porcine (Wilschut et al., 2008) and human muscle (Meng et al., 2011). To our knowledge, this is the first paper describing the purification of murine muscle cells with the NCAM-CD56

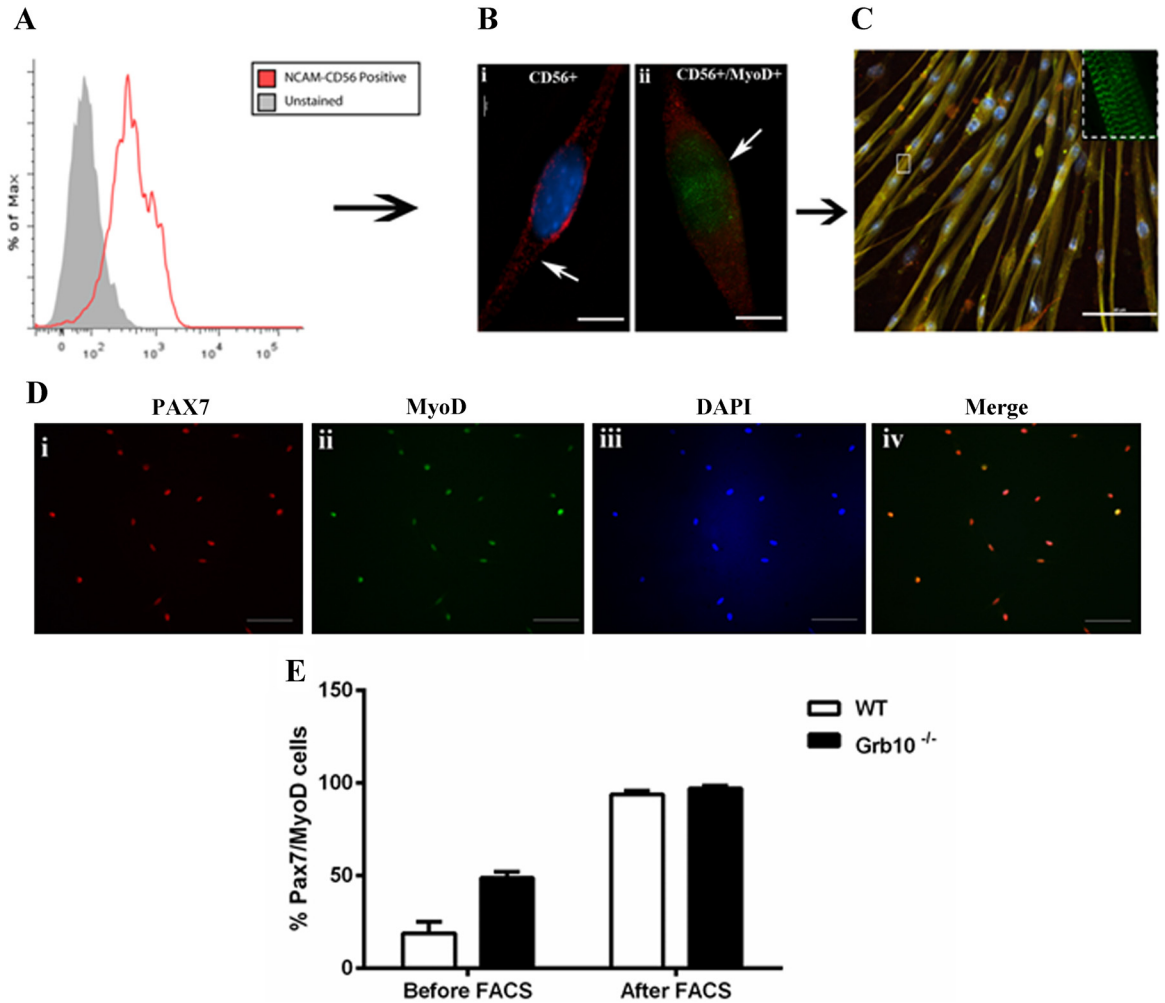

Fig. 2. Isolation of a highly myogenic population of primary muscle cells using NCAM/CD56 cell surface marker. A) Positive staining for NCAM/CD56 in primary murine muscle cells is shown on the histogram by a right shift (red peak) compared to unstained cells (grey peak). B) (i) isolated NCAM/CD56 positive cells (red surface stain, arrow) are elongated in shape with a high nuclear to cytoplasmic ratio and (ii) co-express MyoD (green nuclear stain, arrow), scale bar 10 μm. C) NCAM/CD56 positive cells differentiate into mature multinucleated myotubes as indicated by the co-expression of myosin heavy chain (yellow) and the Z-line marker α-actinin-2 (inset-striated pattern), scale bar 50 μm. D) Representative image from WT primary myoblasts following sorting with NCAM/CD56 antibody showing that the majority of isolated cells are (i) Pax7 positive and (ii) MyoD positive when compared to (iii) total number of nuclei. (iv) Merged image. Scale bar 50 μm. E) Histogram representing percentage of PAX7 positive cells before and after purification with NCAM/CD56 antibody (n = 3 WT & 3 Grb10$^{-/-}$ clones, three independent experiments).

marker. FACS analysis demonstrates that NCAM/CD56 is expressed in mouse primary muscle cells (Fig. 2A, red peak). The isolated NCAM/CD56 positive population consists of spindle-shaped cells with a reduced cytoplasmic volume typical of satellite cells (Fig. 2B.i), and express the myogenic transcription factor MyoD (Fig. 2B.ii), indicating that these cells are actively proliferating. Differentiation of WT and Grb10$^{-/-}$ NCAM/CD56 positive cells in low serum conditions (3% horse serum) results in mature multinucleated primary myotubes as revealed by the striation pattern for α-actinin2 (z-line marker) (Fig. 2C, inset). To verify the purity of sorted cells, immunofluorescence against PAX7 and MyoD was performed (Fig. 2D.i&ii) and the percentage of PAX7/MyoD positive cells determined (Fig. 2D.iv), confirming that our method results in >95% purity (Fig. 2E). The fact that these cells co-express MyoD indicates that they have been activated in culture. Therefore, they will be referred to as activated satellite cells or primary myoblasts henceforth.

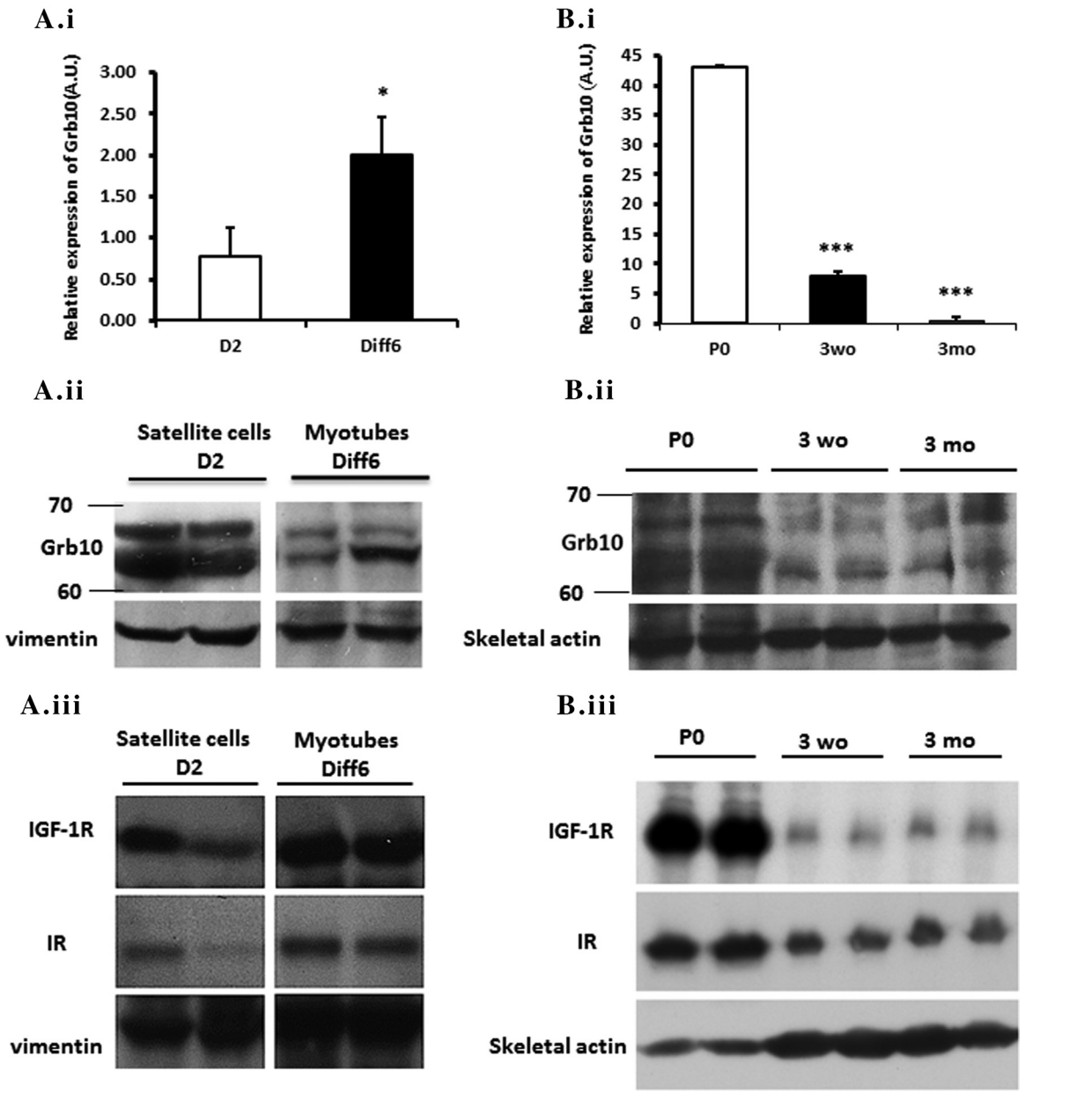

Fig. 3. Grb10 is present in primary myoblasts and differentiated myotubes and is developmentally regulated in vivo. A) (i) Quantitative PCR (qPCR) analysis showing expression of Grb10 mRNA in WT day 2 (D2) myoblasts and day 6 differentiated myotubes (Diff6) relative to cyclophilin (n = 3 WT, three independent experiments, *$P < 0.05$, *t*-test). (ii) Grb10 was also detected at the protein level in D2 myoblasts and Diff6 myotubes. (iii) Expression profile of IGF-1R & IR in WT myoblasts and myotubes. B) (i) qPCR and (ii) Western blot analysis show that Grb10 is highly expressed in new born pup muscle (P0) with levels decreasing as the muscle matures (3 wo, 3 mo), (n = 3 WT from each time point, two independent experiments, ***$P < 0.001$, *t*-test), (iii) Expression profile of IGF-1R and IR in muscle from mice at stage P0, 3 wo and 3 mo.

Grb10 is expressed in activated satellite cells and expression levels in skeletal muscle decrease with muscle maturity

To ascertain the expression of Grb10 in primary myoblasts and differentiated myotubes in vitro, and to determine the expression levels of Grb10 in maturing muscle in vivo, qPCR and Western blot analysis were performed. Both methods demonstrated that Grb10 is expressed in primary myoblasts (D2) and differentiated myotubes (Diff6) in vitro (Fig. 3A.i&ii). In vivo, Grb10 appeared to be developmentally regulated with highest Grb10 expression levels detected by qPCR and immunoblot in muscle of newborn pups and lower levels in 3 week old mice and 3 month old mice (Fig. 3B.i&ii). Two known binding partners of Grb10, the IR and the IGF-1R, are also expressed in myoblasts and myotubes (Fig. 3A.iii). In muscle tissue, the expression pattern of these receptors parallels that of Grb10 (Fig. 3B.iii).

Grb10 deletion enhances proliferation of primary muscle cells and alters the expression of key cell cycle markers

To investigate the proliferative capacity of Grb10$^{-/-}$ primary myoblasts, we examined the mean population doubling time using both a manual cell count and BrdU incorporation assay. After 48 h in culture, more Grb10$^{-/-}$ primary myoblasts were detected compared to WT (Fig. 4A.i&ii). Manual cell count demonstrated a twofold increase in Grb10$^{-/-}$ cell number

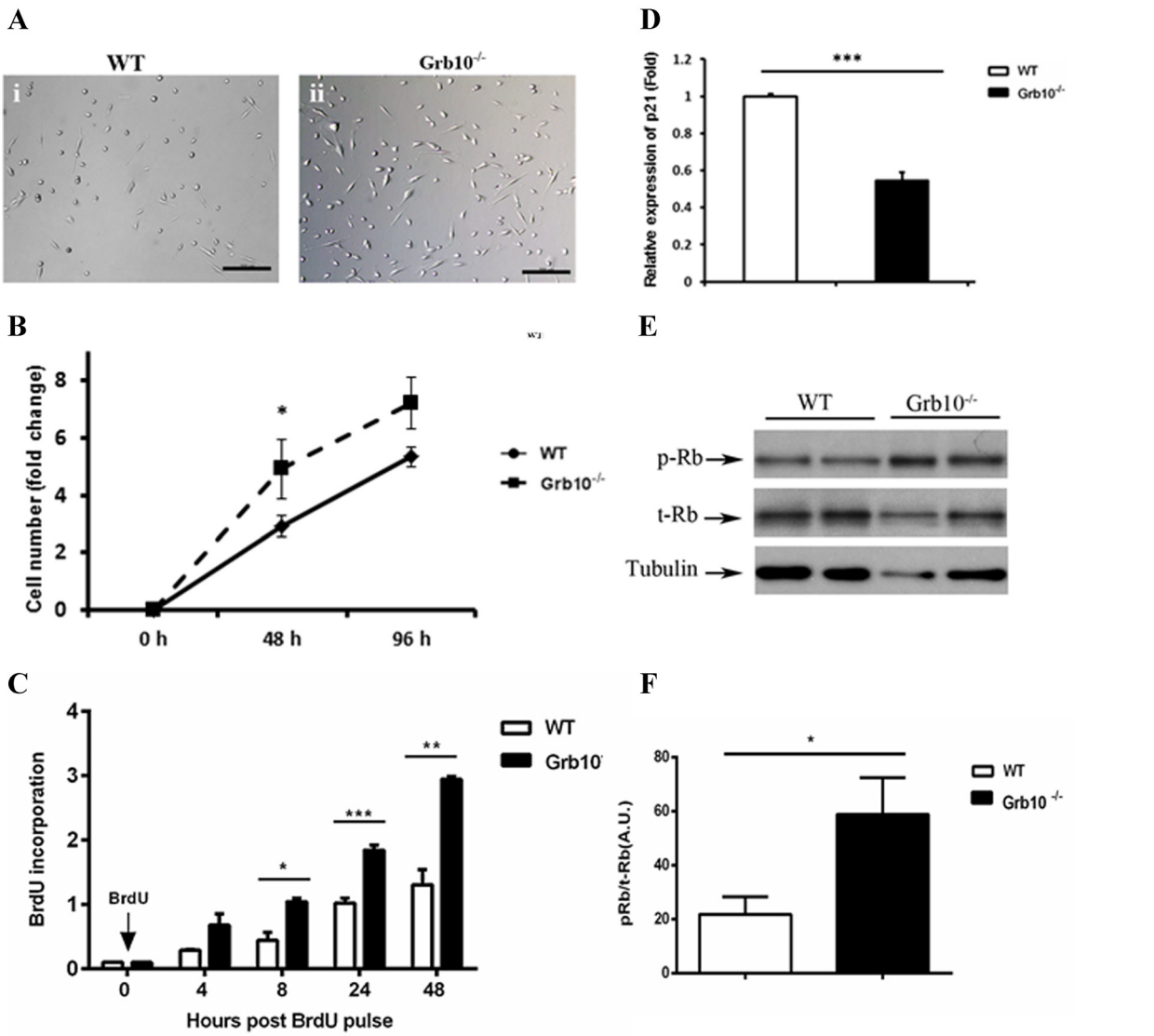

Fig. 4. Absence of Grb10 enhances muscle cell proliferation and alters the expression of key cell cycle markers. A) Brightfield images showing a larger number of (ii) Grb10$^{-/-}$ cells compared to (i) WT after 48 h in culture, scale bar 50 m. B) Manual cell count of WT and Grb10$^{-/-}$ cells at 48 and 96 h. C) BrdU incorporation at 8, 24, and 48 h (n = 3 WT & Grb10$^{-/-}$ clones, three independent experiments, *P<0.05, **P<0.01, ***P < 0.001, t-test). D) qPCR analysis of p21 mRNA (n = 3 WT & 3 Grb10$^{-/-}$ clones, three independent experiments, ***P < 0.001, t-test) E) Representative Western blots from WT & Grb10$^{-/-}$ protein lysates at 48 h blotted for p-Rb and total Rb. F) densitometry analysis of p-Rb in Grb10$^{-/-}$ myoblasts compared to WT when normalised to total levels of Rb (t-Rb) (n = 3 WT & 3 Grb10$^{-/-}$ clones, two independent experiments, *P < 0.05, t-test).

(Fig. 4B, $P < 0.05$) that was also confirmed by the BrdU assay showing a significant increase in BrdU incorporation at 8, 24, and 48 h after pulsing with BrdU (Fig. 4C). To further understand the molecular mechanisms leading to the increase in cell proliferation, we measured markers of the G1-S cell cycle checkpoint; namely p21 and its downstream target retinoblastoma protein (Rb). qPCR analysis showed a significant decrease in p21 transcript levels in D2 Grb10$^{-/-}$ myoblasts (Fig. 4D, $P < 0.001$) which was associated with a twofold increase in phosphorylation of Rb (pRb) (Fig. 4E&F, $P < 0.05$).

Grb10 deletion enhances Akt and ERK signaling in primary myoblasts

To investigate a role for Grb10 in primary myoblast signaling, we examined phosphorylation of the mitogenic signaling pathway targets Akt and ERK. Following insulin stimulation, there was no significant difference in the response between WT and Grb10$^{-/-}$ myoblasts for either p-Akt or p-ERK (Fig. 5A). However, a modest difference in the phosphorylation of these signaling proteins was observed between the two genotypes in the basal state (growth factor-free media). To test the response to well-established myogenic growth factors, stimulation with IGF-1 and HGF was also performed. WT myoblasts were responsive, with increased phosphorylation of Akt and ERK in the presence of growth factors compared to the basal state (1.8- or 7-fold increase of p-ERK for IGF-1 or HGF respectively, and 2.9- or 2.6-fold increase of p-Akt for IGF-1 or HGF respectively) (Fig. 5B). No significant difference was detected in the levels of p-ERK and p-Akt between WT and Grb10$^{-/-}$ myoblasts following stimulation by either IGF-1 or HGF (Fig. 5B). However, markedly higher levels of phosphorylation of ERK (1/2) (p-ERK) and Akt (p-Akt) were again seen in the basal state in Grb10$^{-/-}$ myoblasts compared to WT (3- and 2.5-fold increase, respectively) (Fig. 5B).

Grb10 deletion produces faster transition to a myogenin-positive state

To better understand the role of Grb10 during muscle differentiation, the expression levels of Grb10 at early time

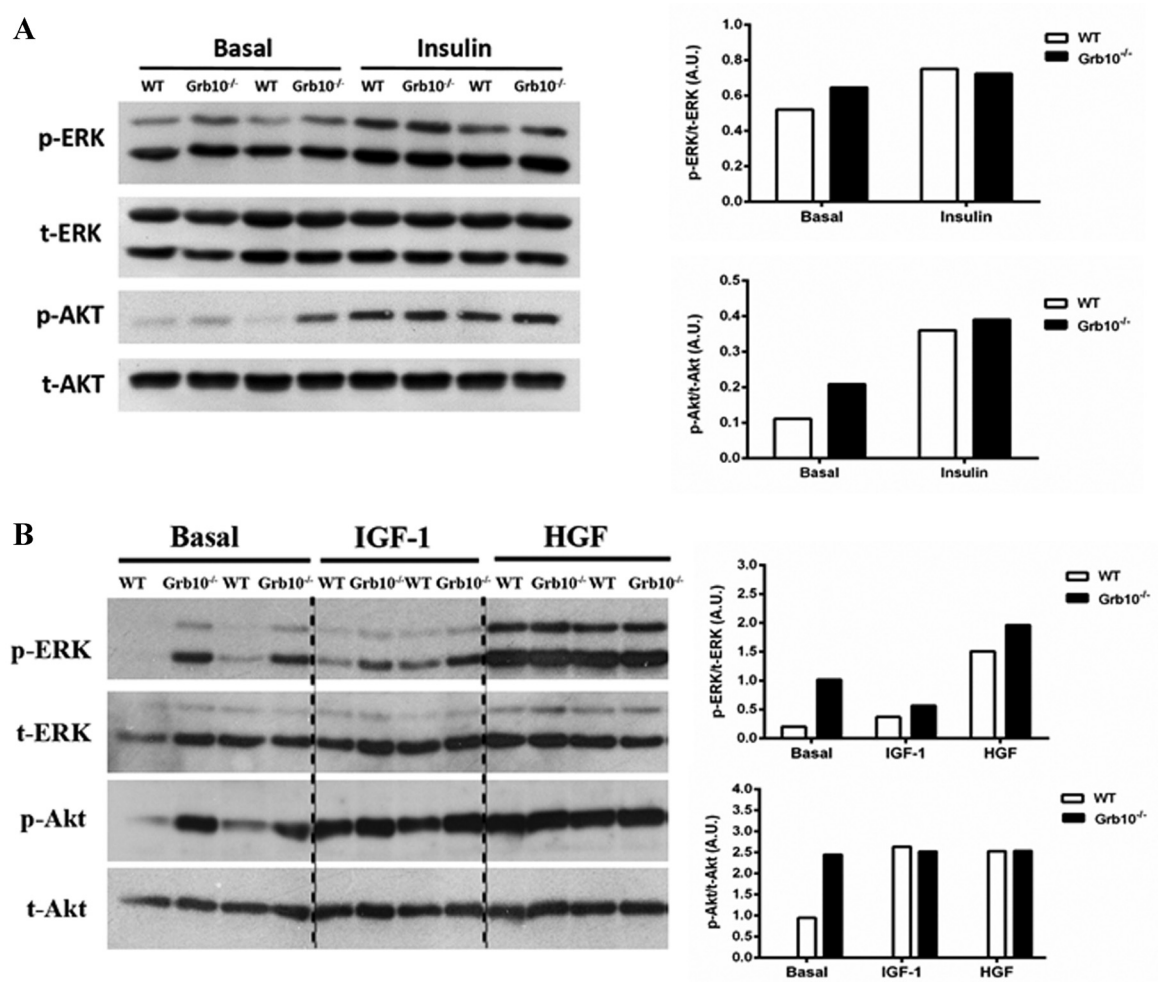

Fig. 5. Absence of Grb10 results in enhanced ERK and Akt signalling at baseline. A) Representative Western blot of ERK(1/2) and Akt on protein lysates extracted from WT and Grb10$^{-/-}$ myoblasts at baseline (6 h of serum starvation) and following insulin stimulation (n = 2 WT, 2 Grb10$^{-/-}$, two independent experiments) with densitometry analysis. B) Representative Western blot of ERK(1/2) and Akt on protein lysates extracted from WT and Grb10$^{-/-}$ myoblasts at baseline (6 h of serum starvation) and following stimulation with IGF-1 or HGF (n = 2 WT, 2 Grb10$^{-/-}$, two independent experiments) with densitometry analysis.

points of myoblast differentiation were determined. To induce differentiation, cells were switched to differentiation media (DM) and mRNA collected from WT cells after 1 (Diff1), 2 (Diff2) and 6 days (Diff6) of differentiation. qPCR showed an increase in the level of Grb10 transcripts in differentiating myoblasts, with levels peaking significantly after 2 days of differentiation (Fig. 6A, $P < 0.05$). Grb10 levels were lower in mature myotubes (Diff6), but similar to previous results, remained higher compared to undifferentiated myoblasts (D2). Morphological assessment of Diff6 Grb10$^{-/-}$ myotubes showed no apparent differences to WT, suggesting that Grb10$^{-/-}$ cells are able to differentiate fully (Fig. 6B.i&ii). To assess the rate of differentiation in WT and Grb10$^{-/-}$myoblasts, subconfluent WT and Grb10$^{-/-}$ myoblasts were switched to DM and pulsed with BrdU at 12, 24 (Diff1), and 48 h (Diff2) of differentiation. The percentage difference in BrdU incorporation relative to cells growing in normal growth media (cells still cycling) was then measured. After 12 h of switching to differentiation media, a 52% decrease in BrdU incorporation was observed in Grb10$^{-/-}$ myoblasts compared to 27% in WT (Fig. 7A.i). A significant decrease in BrdU incorporation was observed at 24 h (Grb10$^{-/-}$ 65%, WT 43%) (Fig. 7A.ii). However, no difference was observed between WT and Grb10$^{-/-}$ cells at 48 h (Diff2) of differentiation(Grb10$^{-/-}$ 64%, WT 66%, Fig. 7A.iii). These results indicate that when induced to differentiate, Grb10$^{-/-}$ myoblasts can exit the cell cycle at a faster rate than WT cells, but only for a short time interval. We then examined the expression levels of myogenin, a marker of early differentiation. Lysates from WT and Grb10$^{-/-}$ differentiating myoblasts were collected 24 h (Diff1) after switching to DM (Fig. 7B), and Western blot analysis of myogenin demonstrated a 2-fold increase in expression levels in Grb10$^{-/-}$ myoblasts compared to WT (Fig. 7C&D).

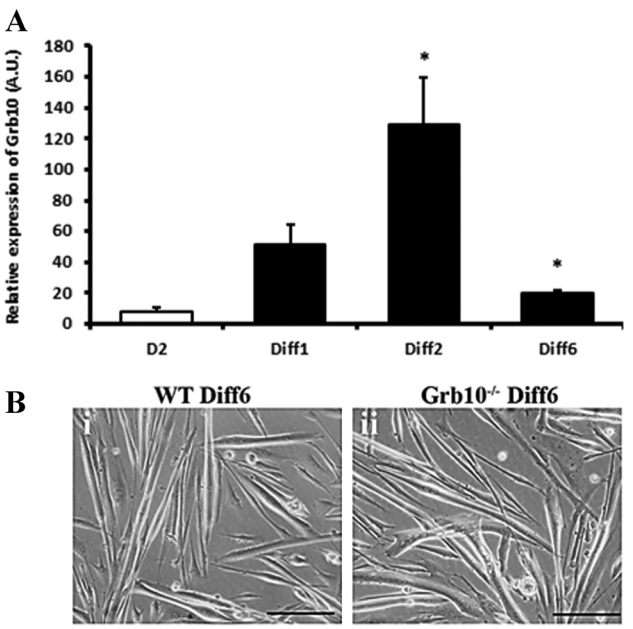

Fig. 6. Grb10 mRNA levels increase during early stages of differentiation but Grb10 is dispensable for the formation of myotubes. A) qPCR analysis of Grb10 mRNA isolated from WT primary myoblasts (D2) and differentiating myotubes (Diff1, Diff2, Diff6) (n = 3 WT & 3 Grb10$^{-/-}$ clones, three independent experiments, *$P < 0.05$, t-test) normalised to cyclophilin. B) Brightfield images of Diff6 (i) WT and (ii) Grb10$^{-/-}$ myotubes, scale bar 50 μm.

Grb10$^{-/-}$ primary myotubes display an increase in glucose metabolism and GLUT4 content at the plasma membrane

We evaluated the potential mechanisms by which Grb10 ablation impacts glucose uptake in muscle. $H^3$2-deoxyglucose uptake in Diff6 differentiated myotubes was measured under basal conditions, and following insulin stimulation. Grb10$^{-/-}$ myotubes showed a 2-fold increase in glucose uptake under both conditions (Fig. 8A) compared to WT. GLUT4 translocation assays were performed to investigate the mechanisms underlying the increase in glucose uptake. Cell surface HA-GLUT4 constituted ~25% of total HA-GLUT4 content in WT myotubes, while in Grb10$^{-/-}$myotubes, it represented 55% (Fig. 8B). No significant difference in surface HA-GLUT4 level was seen between WT and Grb10$^{-/-}$ myotubes following insulin stimulation. Signaling pathways were also examined. In the basal state, there was a tendency for higher levels of p-ERK and p-Akt in Grb10$^{-/-}$ myotubes, and the same was found following insulin stimulation (Fig. 8C,D).

Discussion

Factors that regulate muscle mass have the potential to offer therapeutical benefits in treating muscle diseases and improving metabolic health. Our laboratory has recently identified Grb10 as one such protein (Holt et al., 2012). In the present study, we developed an in vitro model of pure primary murine muscle cells to investigate the mode of action of Grb10 and provide insight into mechanisms that contribute to the growth of muscle mass and the phenotype of improved insulin action observed for Grb10 KO mice in vivo.

The satellite cell population in skeletal muscle is also referred to as adult muscle stem cells. As well as having a common origin with embryonic muscle precursor cells, they share many cellular and molecular features, making them an appropriate model for the study of muscle development in vitro. However, such investigations require isolation of a highly pure population of satellite cells to be able to specifically evaluate muscle cell proliferation, differentiation, and intracellular signaling cascades. Here, we provide a method combining explant isolation with FACS to specifically enrich for muscle satellite cells. To date, only two cell surface markers (CD34 and alpha 7 integrin) have been used to purify mouse muscle cells using FACS (Cooper et al., 1999; Beauchamp et al., 2000; Ieronimakis et al., 2010). Based on studies using human muscle (Meng et al., 2011), we investigated the use of NCAM/CD56 as a marker for the isolation of muscle progenitor cells from mouse tissue. NCAM/CD56 was initially considered as a marker of Natural Killer (NK) cells (Hercend et al., 1985; Jacobs et al., 1992) and later identified to be expressed in a variety of tissues including brain, nerve, and muscle (McClain and Edelman, 1982; Cunningham et al., 1987). We have shown that NCAM/CD56 is expressed on primary muscle cells from mouse tissue. Sorting with this marker yielded over 95% PAX7/MyoD positive cells that can actively engage in the terminal differentiation program (Fig. 2C). To our knowledge, this is the first paper describing the isolation of a pure and highly myogenic population of primary myoblasts from mouse tissue using this marker. Furthermore, we have demonstrated the utility of this method for application to a genetically modified mouse model, to facilitate comparative studies of satellite cell function. We suggest that NCAM/CD56 cell surface marker can be considered by itself or in combination with other established markers when isolating primary muscle cells from mice.

While the role of Grb10 has been previously studied in the context of adult muscle function, its role in myogenesis has been unclear. We demonstrated that Grb10 protein is more

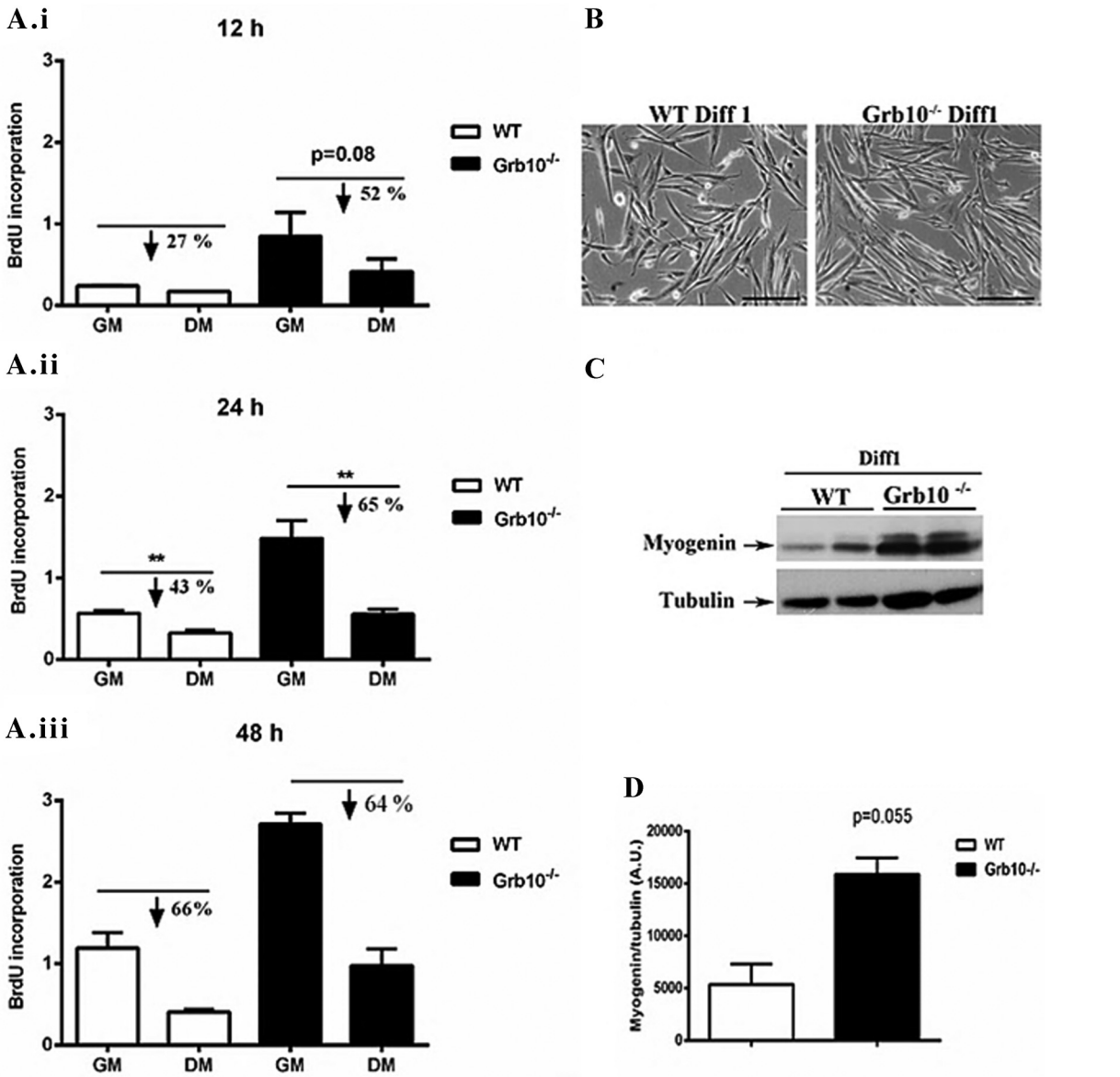

Fig. 7. Deletion of Grb10 produces faster transition to a myogenin-positive state. A) Assessment of the difference in BrdU incorporation after (i) 12 h, (ii) 24 h and (iii) 48 h of switching from growth media (GM) to differentiation media (DM) (n = 3 WT & three Grb10$^{-/-}$, two independent experiments, **$P < 0.01$, ***$P < 0.001$, *t*-test). B) (i) Representative bright field images of Diff1 WT and Grb10$^{-/-}$ differentiating myotubes, scale bar 50 μm. (ii) Western blotting of myogenin on protein lysates extracted from Diff1 WT and Grb10$^{-/-}$ myotubes. (iii) Densitometry analysis of myogenin in WT and Grb10$^{-/-}$ Diff1 myotubes ($P = 0.055$, n = 3 WT & three Grb10$^{-/-}$, two independent experiments).

highly expressed in activated satellite cells than in differentiated myotubes. mRNA level did not correlate with protein, but this could be attributable to post-transcriptional and/or post-translational regulation of Grb10 (Hsu et al., 2011; Yu et al., 2011). In addition, we showed in vivo that in skeletal muscle, the highest expression for Grb10 mRNA and protein is at birth (P0), and these levels significantly decrease during muscle maturation to adulthood (3 months). These results are consistent with previous work showing that Grb10 transcripts, as well as other imprinted genes, are downregulated in adult muscle compared to postnatal day five (P5) skeletal muscle (Berg et al., 2011). The decline in Grb10 expression levels from the postnatal to adult period may also be associated with a drop in the proportion of satellite cells during postnatal muscle growth. At birth, satellite cells represent ~30% of myocyte nuclei, while they only constitute ~2%–7% of nuclei within adult skeletal muscle (Hawke and Garry, 2001; Halevy et al., 2004). Taken together, these results suggest that the expression of this imprinted gene is retained in satellite cells and support a role for Grb10 in early muscle development and satellite cell function.

The hypermuscular phenotype of Grb10$^{-/-}$ mice is related to an increase in muscle fiber number with no apparent changes in fiber size or fiber type proportion (Holt et al., 2012). Fiber number is thought to be established by birth (Ontell and Kozeka, 1984) and is dependent on the number of available

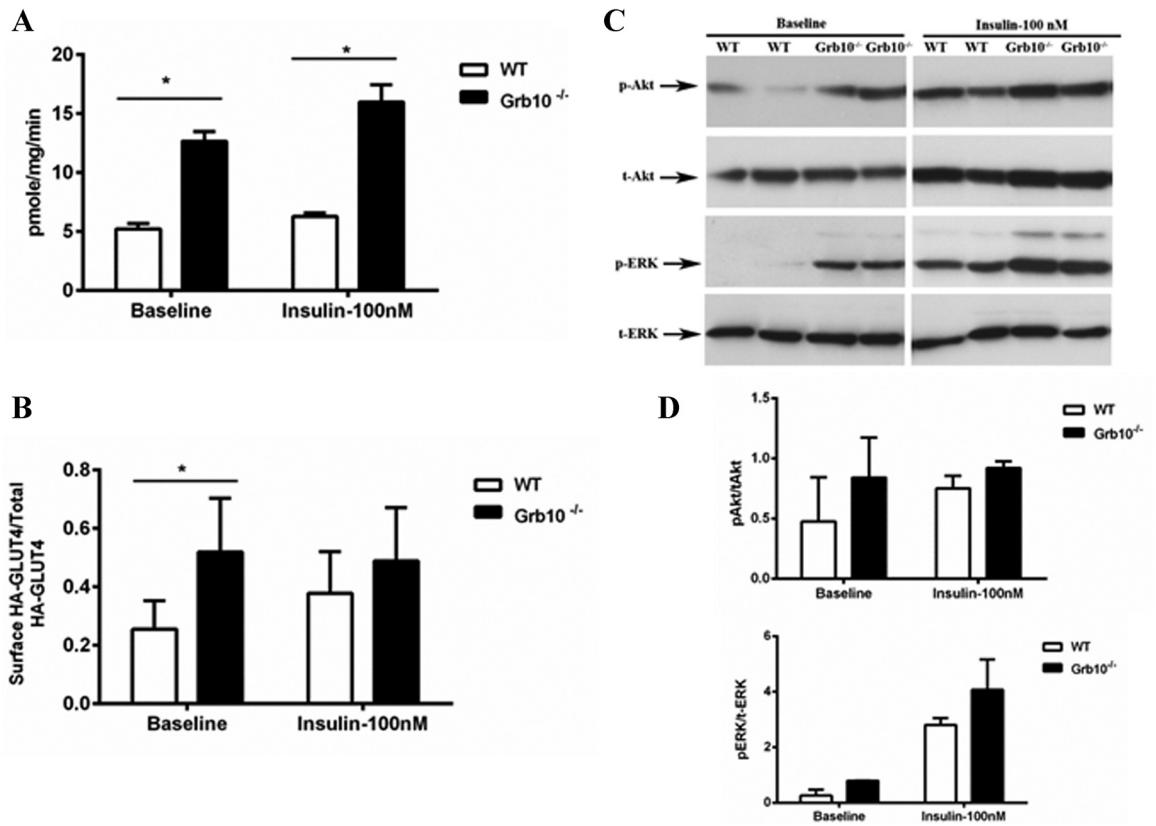

Fig. 8. Ablation of Grb10 results in an increase in glucose metabolism and insulin action A) Glucose uptake assay in WT and Grb10$^{-/-}$ myotubes at baseline and following insulin stimulation (n = 3 WT & 3 Grb10$^{-/-}$ clones, *$P < 0.05$, 2 way Anova, five independent experiments). B) Level of GLUT4 at the membrane at baseline (*$P < 0.05$, *t*-test) and following insulin stimulation. C) Representative Western blot of signalling targets Akt and ERK at baseline and following insulin stimulation in Grb10$^{-/-}$ and WT myotubes. D) Densitometry analysis of p-Akt and p-ERK in Grb10$^{-/-}$ and WT myotubes (n = 2 WT & 2 Grb10$^{-/-}$ clones).

myogenic progenitor cells. Therefore, we hypothesized that the increase in fiber number is likely due to an increase in the proliferation of muscle progenitor cells during early stages of muscle development. Studies have shown both positive (O'Neill et al., 1996; Wang et al., 1999) and negative (Liu and Roth, 1995; Morrione et al., 1997) roles for Grb10 in regulating cellular proliferation. However, it is possible that these differences result from the different cellular model examined or the differences in experimental procedure. Our results demonstrate that Grb10 acts as a negative regulator of muscle cell proliferation. We show that Grb10$^{-/-}$ primary muscle cells proliferate faster than WT cells by transitioning rapidly from the G0 to the S (DNA synthesis) phase of the cell cycle. Molecularly, the increased proliferative capacity of Grb10$^{-/-}$ cells was associated with downregulation of p21 transcript levels and hyperphosphorylation of Rb. Changes in p21 levels and Rb activity are known to affect cell cycle dynamics, with upregulation of p21 being associated with permanent cell cycle arrest of muscle cells (Nevins, 1992; Sherr, 1996; Walsh et al., 1996), whilst phosphorylation of Rb releases E2F from the complex to enhance transition through the cell cycle (Gottifredi et al., 2004). Our findings provide compelling evidence that ablation of Grb10 in muscle cells stimulates the proliferative potential. They are also consistent with those described for myostatin ablated mice (myostatin$^{-/-}$) where the increase in muscle mass was associated with an enhanced proliferative capacity of satellite cells and changes in cell cycle markers (McPherron et al., 1997; Joulia et al., 2003; McCroskery et al., 2003).

In addition to the changes we observed in cell cycle markers, we also demonstrated that absence of Grb10 affects upstream proteins in proliferation signaling pathways including Akt and ERK. Phosphorylation of both Akt and ERK is markedly enhanced in Grb10$^{-/-}$ myoblasts in the basal state. Stimulation with growth factors IGF-1 or HGF in Grb10$^{-/-}$ myoblasts did not further increase phosphorylation of these targets indicating that Grb10$^{-/-}$ cells are near maximal phosphorylation even under basal conditions. It is not known which signaling molecules upstream of Akt and ERK are activated to maintain this phosphorylation in the basal state, nor which growth factor receptor is likely to be involved in triggering these effects. Grb10 has an established role in binding the IR and IGFR (Liu and Roth, 1995; Morrione et al., 1996; O'Neill et al., 1996; Laviola et al., 1997; Ramos et al., 2006). Moreover there is some evidence from in vitro studies showing that Grb10 binds to FGFR and HGFR (Wang et al., 1999). Therefore it is likely that any one or all of these growth factor receptors are residually activated and could be involved in the enhanced basal activation of Akt and ERK when the Grb10 interaction is abolished.

In addition to the increase in cell proliferation, our data demonstrate that Grb10 does not affect the ability of myoblasts

to differentiate, but rather impacts on when terminal differentiation is initiated. Grb10 transcript levels peak during early time points of differentiation suggesting that Grb10 may be required to initiate differentiation. However, Grb10$^{-/-}$ myoblasts do differentiate and form functional myotubes similar in morphology and size to WT myotubes. It is known that terminal differentiation requires permanent withdrawal from cell cycle and is regulated by the expression of the early differentiation marker myogenin (Kitzmann and Fernandez, 2001). Our studies from the BrdU labeling experiments show that Grb10$^{-/-}$ myoblasts withdraw faster from the cell cycle compared to WT. In addition, the molecular basis for the increased withdrawal is due to an early increase in the expression levels of myogenin. Taken together, these results provide evidence that absence of Grb10 does not directly modify the differentiation program; but rather provides an environment that facilitates a faster differentiation of myoblasts to myotubes. Based on the proliferation and differentiation data presented here, we propose Grb10 as a regulator of distinct intracellular signaling pathways involved in both proliferation and differentiation of primary myoblasts.

Previous studies have demonstrated that Grb10-ablated mice have an improved insulin action and improved whole body glucose homeostasis compared to WT mice (Smith et al., 2007; Wang et al., 2007). To investigate whether Grb10 ablation has a direct effect on muscle cell metabolism, glucose uptake was investigated in differentiated myotubes from WT and Grb10$^{-/-}$ cells. Our results demonstrated that Grb10$^{-/-}$ myotubes have a twofold higher glucose uptake in the basal state compared to WT. This improved glucose uptake in Grb10$^{-/-}$ myotubes was accompanied by an increase in GLUT4 transporters at the plasma membrane and a tendency toward an enhanced Akt and ERK signaling. Reduced GLUT4 translocation to the plasma membrane is thought to be a major contributor to the defect in glucose transport in skeletal muscles of insulin resistant and type 2 diabetic patients (Ryder et al., 2000). Therefore, these results provide further evidence that lack of Grb10 enhances insulin signaling and glucose transport in myotubes in vitro and supports in vivo data suggesting that improved insulin action in Grb10$^{-/-}$ mice may be due to differences in muscle metabolism.

Myoblast proliferation and differentiation are early critical processes that regulate muscle growth and also regeneration. A defect in satellite cell proliferation or differentiation is associated with different metabolic diseases including type II diabetes and obesity, as well as with muscular diseases and with reduced muscle mass during aging (Allbrook et al., 1971; Purchas et al., 1985; Mozdziak et al., 1994; Aguiari et al., 2008). In the current study, we developed and utilized an in vitro model of highly purified primary muscle cells to study mechanisms of action of Grb10 in muscle cells. We provide evidence supporting a role for Grb10 as a factor that regulates the balance between muscle cell proliferation and differentiation via modulating signaling pathways and expression of key cell cycle and differentiation markers (Fig. 9). In addition, we demonstrated that absence of Grb10 increases glucose uptake via enhanced translocation of GLUT4 transporters to the plasma membrane. These data identify Grb10 as a potential therapeutical target to improve glucose metabolism and alleviate the reduction in muscle mass associated with muscle disorders and aging.

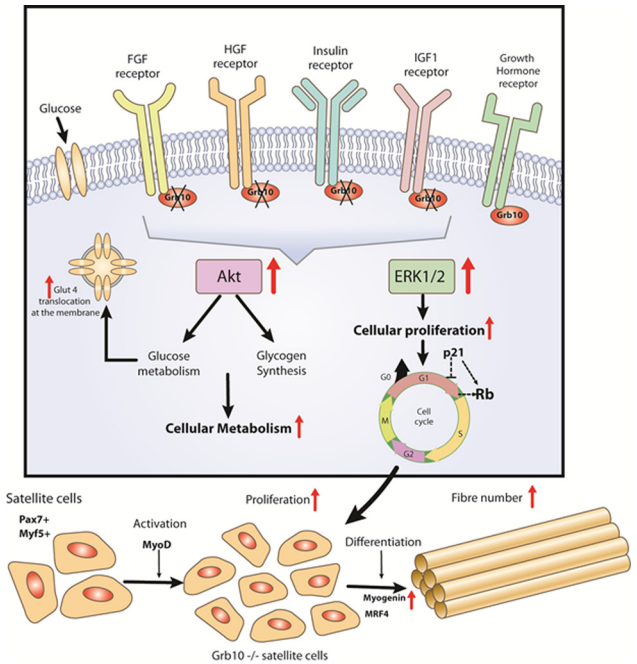

Fig. 9. A model for the role of Grb10 in muscle cell proliferation and glucose metabolismAbsence of Grb10 results in an enhanced growth factor signaling leading to increase in Akt and ERK activity. The downstream effect of ERK is an increase in cell proliferation through regulation of key cell cycle markers (p21 and Rb). In addition, enhanced Akt activity leads to an improved glucose metabolism and insulin action.

Acknowledgments

The authors thank the Flow Cytometry Facility team at the Garvan Institute, Robert Solomon and David Snowden, for their assistance with the FACS experiments and Brendan Roome for his assistance with the Adobe Illustrator program. We also thank Amanda Brandon and Kim Moran-Jones from the Garvan Institute for their review of the manuscript. The hybridoma antibodies: PAX7, Myogenin, β-tubulin, and myosin chain were respectively developed by investigators Atsushi Kawakami, Klymkowsky, M., Wright, W.E., Fischman, D.A. and were obtained from the Developmental Studies Hybridoma Bank developed under the auspices of the NICHD and maintained at The University of Iowa. This work was supported by funding from the National Health and Medical Research Council (NHMRC) of Australia (481335). C.M.G. received salary support from a postgraduate scholar award (APA) from the University of Sydney. N.T. is supported by an Australian Research Council Future Fellowship. G.J.C and R.J.D are supported by research fellowships, from the NHMRC of Australia. The authors declare no conflicts of interest.

Literature Cited

Aguiari P, Leo S, Zavan B, Vindigni V, Rimessi A, Bianchi K, Franzin C, Cortivo R, Rossato M, Vettor R, Abatangelo G, Pozzan T, Pinton P, Rizzuto R. 2008. High glucose induces adipogenic differentiation of muscle-derived stem cells. Proc Natl Acad Sci USA 105:1226–1231.

Allbrook DB, Han MF, Hellmuth AE. 1971. Population of muscle satellite cells in relation to age and mitotic activity. Pathology 3:223–243.

Beauchamp JR, Heslop L, Yu DS, Tajbakhsh S, Kelly RG, Wernig A, Buckingham ME, Partridge TA, Zammit PS. 2000. Expression of CD34 and Myf5 defines the majority of quiescent adult skeletal muscle satellite cells. J Cell Biol 151:1221–1234.

Bendall SC, Stewart MH, Menendez P, George D, Vijayaragavan K, Werbowetski-Ogilvie T, Ramos-Mejia V, Rouleau A, Yang J, Bosse M, Lajoie G, Bhatia M. 2007. IGF and FGF cooperatively establish the regulatory stem cell niche of pluripotent human cells in vitro. Nature 448:1015–1021.

Berg JS, Lin KK, Sonnet C, Boles NC, Weksberg DC, Nguyen H, Holt LJ, Rickwood D, Daly RJ, Goodell MA. 2011. Imprinted genes that regulate early mammalian growth are coexpressed in somatic stem cells. PloS One 6:e26410.

Bischoff R. 1990. Control of satellite cell proliferation. Adv Exp Med Biol 280:147–157.

Charalambous M, Smith FM, Bennett WR, Crew TE, Mackenzie F, Ward A. 2003. Disruption of the imprinted Grb10 gene leads to disproportionate overgrowth by an Igf2-independent mechanism. Proc Natl Acad Sci USA 100:8292–8297.

Coleman ME, DeMayo F, Yin KC, Lee HM, Geske R, Montgomery C, Schwartz RJ. 1995. Myogenic vector expression of insulin-like growth factor I stimulates muscle cell differentiation and myofiber hypertrophy in transgenic mice. J Biol Chem 270:12109–12116.

Cooper RN, Tajbakhsh S, Mouly V, Cossu G, Buckingham M, Butler-Browne GS, In vivo satellite cell activation via Myf5 and MyoD in regenerating mouse skeletal muscle J Cell Sci 1121999; 2895–2901.

Cruz Guzman Odel R, Chavez Garcia AL, Rodriguez-Cruz M. 2012. Muscular dystrophies at different ages: Metabolic and endocrine alterations. Int J Endocrinol 2012:485376.

Cunningham BA, Hemperly JJ, Murray BA, Prediger EA, Brackenbury R, Edelman GM. 1987. Neural cell adhesion molecule: Structure, immunoglobulin-like domains, cell surface modulation, and alternative RNA splicing. Science 236:799–806.

Decary S, Mouly V, Hamida CB, Sautet A, Barbet JP, Butler-Browne GS. 1997. Replicative potential and telomere length in human skeletal muscle: Implications for satellite cell-mediated gene therapy. Hum Gene Ther 8:1429–1438.

DeFronzo RA, Gunnarsson R, Bjorkman O, Olsson M, Wahren J. 1985. Effects of insulin on peripheral and splanchnic glucose metabolism in noninsulin-dependent (type II) diabetes mellitus. J Clin Invest 76:149–155.

Duclos MJ, Wilkie RS, Goddard C. 1991. Stimulation of DNA synthesis in chicken muscle satellite cells by insulin and insulin-like growth factors: Evidence for exclusive mediation by type-I insulin-like growth factor receptor.. J Endocrinol 128:35–42.

Evans W. 1997. Functional and metabolic consequences of sarcopenia. J Nutr 127:998S–1003S.

Gottifredi V, McKinney K, Poyurovsky MV, Prives C. 2004. Decreased p21 levels are required for efficient restart of DNA synthesis after S phase block. J Biol Chem 279:5802–5810.

Govers R, Coster AC, James DE. 2004. Insulin increases cell surface GLUT4 levels by dose dependently discharging GLUT4 into a cell surface recycling pathway. Mol Cell Biol 24:6456–6466.

Gros J, Manceau M, Thome V, Marcelle C. 2005. A common somitic origin for embryonic muscle progenitors and satellite cells. Nature 435:954–958.

Halevy O, Piestun Y, Allouh MZ, Rosser BW, Rinkevich Y, Reshef R, Rozenboim I, Wleklinski-Lee M, Yablonka-Reuveni Z. 2004. Pattern of Pax7 expression during myogenesis in the posthatch chicken establishes a model for satellite cell differentiation and renewal. Dev Dyn 231:489–502.

Hawke TJ, Garry DJ. 2001. Myogenic satellite cells: physiology to molecular biology. J Appl Physiol 91:534–551.

Hercend T, Griffin JD, Bensussan A, Schmidt RE, Edson MA, Brennan A, Murray C, Daley JF, Schlossman SF, Ritz J. 1985. Generation of monoclonal antibodies to a human natural killer clone. Characterization of two natural killer-associated antigens, NKH1A and NKH2, expressed on subsets of large granular lymphocytes. J Clin Invest 75:932–943.

Holt LJ, Lyons RJ, Ryan AS, Beale SM, Ward A, Cooney GJ, Daly RJ. 2009. Dual ablation of Grb10 and Grb14 in mice reveals their combined role in regulation of insulin signaling and glucose homeostasis. Mol Endocrinol 23:1406–1414.

Holt LJ, Siddle K, Grb10 and Grb14: enigmatic regulators of insulin action—and more? Biochem J 3882005; 393–406.

Holt LJ, Turner N, Mokbel N, Trefely S, Kanzleiter T, Kaplan W, Ormandy CJ, Daly RJ, Cooney GJ. 2012. Grb10 regulates the development of fiber number in skeletal muscle. FASEB J 26:3658–3669.

Hoy AJ, Bruce CR, Cederberg A, Turner N, James DE, Cooney GJ, Kraegen EW. 2007. Glucose infusion causes insulin resistance in skeletal muscle of rats without changes in Akt and AS160 phosphorylation. Am J Physiol Endocrinol Metab 293:E1358–E1364.

Hsu PP, Kang SA, Rameseder J, Zhang Y, Ottina KA, Lim D, Peterson TR, Choi Y, Gray NS, Yaffe MB, Marto JA, Sabatini DM. 2011. The mTOR-regulated phosphoproteome reveals a mechanism of mTORC1-mediated inhibition of growth factor signaling. Science 332:1317–1322.

Ieronimakis N, Balasundaram G, Rainey S, Srirangam K, Yablonka-Reuveni Z, Reyes M. 2010. Absence of CD34 on murine skeletal muscle satellite cells marks a reversible state of activation during acute injury. PloS One 5:e10920.

Ilkovski B, Nowak KJ, Domazetovska A, Maxwell AL, Clement S, Davies KE, Laing NG, North KN, Cooper ST. 2004. Evidence for a dominant-negative effect in ACTA1 nemaline myopathy caused by abnormal folding, aggregation and altered polymerization of mutant actin isoforms. Hum Mol Genet 13:1727–1743.

Jacobs RSM, Stratmann G, Leo R, Link H, Schmidt RE. 1992. CD16- CD56+ natural killer cells after bone marrow transplantation. Blood Coagul Fibrinolysis 79:3239–3244.

Janssen I, Heymsfield SB, Wang ZM, Ross R. 2000. Skeletal muscle mass and distribution in 468 men and women aged 18–88 yr. J Appl Physiol (1985) 89:81–88.

Joulia D, Bernardi H, Garandel V, Rabenoelina F, Vernus B, Cabello G. 2003. Mechanisms involved in the inhibition of myoblast proliferation and differentiation by myostatin. Exp Cell Res 286:263–275.

Kitzmann M, Fernandez A. 2001. Crosstalk between cell cycle regulators and the myogenic factor MyoD in skeletal myoblasts. Cell Mol Life Sci 58:571–579.

Laviola L, Giorgino F, Chow JC, Baquero JA, Hansen H, Ooi J, Zhu J, Riedel H, Smith RJ. 1997. The adapter protein Grb10 associates preferentially with the insulin receptor as compared with the IGF-I receptor in mouse fibroblasts. J Clin Invest 99:830–837.

Le Grand F, Rudnicki MA. 2007. Skeletal muscle satellite cells and adult myogenesis. Curr Opin Cell Biol 19:628–633.

Liu BA, Engelmann BW, Jablonowski K, Higginbotham K, Stergachis AB, Nash PD. 2012. SRC Homology 2 Domain Binding Sites in Insulin, IGF-1 and FGF receptor mediated signaling networks reveal an extensive potential interactome. Cell Commun Signal 10:27.

Liu F, Roth RA. 1995. Grb-IR: a SH2-domain-containing protein that binds to the insulin receptor and inhibits its function. Proc Natl Acad Sci USA 92:10287–10291.

Maina F, Casagranda F, Audero E, Simeone A, Comoglio PM, Klein R, Ponzetto C. 1996. Uncoupling of Grb2 from the Met receptor in vivo reveals complex roles in muscle development. Cell 87:531–542.

McClain DA, Edelman GM. 1982. A neural cell adhesion molecule from human brain. Proc Natl Acad Sci USA 79:6380–6384.

McCroskery S, Thomas M, Maxwell L, Sharma M, Kambadur R. 2003. Myostatin negatively regulates satellite cell activation and self-renewal. J Cell Biol 162:1135–1147.

McFarland DC, Pesall JE, Gilkerson KK. 1993. The influence of growth factors on turkey embryonic myoblasts and satellite cells in vitro. Gen Comp Endocrinol 89:415–424.

McPherron AC, Lawler AM, Lee SJ. 1997. Regulation of skeletal muscle mass in mice by a new TGF-beta superfamily member. Nature 387:83–90.

Meng J, Adkin CF, Xu SW, Muntoni F, Morgan JE. 2011. Contribution of human muscle-derived cells to skeletal muscle regeneration in dystrophic host mice. PloS One 6:e17454.

Morrione A, Valentinis B, Li S, Ooi JY, Margolis B, Baserga R. 1996. Grb10: A new substrate of the insulin-like growth factor I receptor. Cancer Res 56:3165–3167.

Morrione A, Valentinis B, Xu SQ, Yumet G, Louvi A, Efstratiadis A, Baserga R. 1997. Insulin-like growth factor II stimulates cell proliferation through the insulin receptor. Proc Natl Acad Sci USA 94:3777–3782.

Mozdziak PE, Schultz E, Cassens RG. 1994. Satellite cell mitotic activity in posthatch turkey skeletal muscle growth. Poult Sci 73:547–555.

Musaro A, McCullagh K, Paul A, Houghton L, Dobrowolny G, Molinaro M, Barton ER, Sweeney HL, Rosenthal N. 2001. Localized Igf-1 transgene expression sustains hypertrophy and regeneration in senescent skeletal muscle. Nat Genet 27:195–200.

Nevins JR. 1992. E2F: A link between the Rb tumor suppressor protein and viral oncoproteins. Science 258:424–429.

O'Neill TJ, Rose DW, Pillay TS, Hotta K, Olefsky JM, Gustafson TA. 1996. Interaction of a GRB-IR splice variant (a human GRB10 homolog) with the insulin and insulin-like growth factor I receptors. Evidence for a role in mitogenic signaling. J Biol Chem 271:22506–22513.

Ontell M, Kozeka K. 1984. Organogenesis of the mouse extensor digitorum logus muscle: a quantitative study. Am J Anat 171:149–161.

Ooi J, Yajnik V, Immanuel D, Gordon M, Moskow JJ, Buchberg AM, Margolis B. 1995. The cloning of Grb10 reveals a new family of SH2 domain proteins. Oncogene 10:1621–1630.

Purchas RW, Romsos DR, Allen RE, Merkel RA. 1985. Muscle growth and satellite cell proliferative activity in obese (OB/OB) mice. J Anim Sci 60:644–651.

Ramos FJ, Langlais PR, Hu D, Dong LQ, Liu F. 2006. Grb10 mediates insulin-stimulated degradation of the insulin receptor: a mechanism of negative regulation. Am J Physiol Endocrinol Metab 290:E1262–E1266.

Ryder JW, Yang J, Galuska D, Rincon J, Bjornholm M, Krook A, Lund S, Pedersen O, Wallberg-Henriksson H, Zierath JR, Holman GD. 2000. Use of a novel impermeable biotinylated photolabeling reagent to assess insulin- and hypoxia-stimulated cell surface GLUT4 content in skeletal muscle from type 2 diabetic patients. Diabetes 49:647–654.

Sabourin LA, Rudnicki MA. 2000. The molecular regulation of myogenesis. Clinical genetics 57:16–25.

Sherr CJ. 1996. Cancer cell cycles. Science 274:1672–1677.

Shewan AM, van Dam EM, Martin S, Luen TB, Hong W, Bryant NJ, James DE. 2003. GLUT4 recycles via a trans-Golgi network (TGN) subdomain enriched in Syntaxins 6 and 16 but not TGN38: involvement of an acidic targeting motif. Mol Biol Cell 14:973–986.

Shulman GI, Rothman DL, Jue T, Stein P, DeFronzo RA, Shulman RG. 1990. Quantitation of muscle glycogen synthesis in normal subjects and subjects with non-insulin-dependent diabetes by 13C nuclear magnetic resonance spectroscopy. N Engl J Med 322:223–228.

Smith FM, Holt LJ, Garfield AS, Charalambous M, Koumanov F, Perry M, Bazzani R, Sheardown SA, Hegarty BD, Lyons RJ, Cooney GJ, Daly RJ, Ward A. 2007. Mice with a disruption of the imprinted Grb10 gene exhibit altered body composition, glucose homeostasis, and insulin signaling during postnatal life. Mol Cell Biol 27:5871–5886.

Srikanthan P, Karlamangla AS. 2011. Relative muscle mass is inversely associated with insulin resistance and prediabetes. Findings from the third National Health and Nutrition Examination Survey. J Clin Endocrinol Metab 96:2898–2903.

Tan SX, Ng Y, James DE. 2010. Akt inhibitors reduce glucose uptake independently of their effects on Akt. Biochem J 432(1):191–197.

Tatsumi R, Anderson JE, Nevoret CJ, Halevy O, Allen RE. 1998. HGF/SF is present in normal adult skeletal muscle and is capable of activating satellite cells. Dev Biol 194:114–128.

Walsh AA, Tullis K, Rice RH, Denison MS. 1996. Identification of a novel cis-acting negative regulatory element affecting expression of the CYP1A1 gene in rat epidermal cells. J Biol Chem 271:22746–22753.

Wang J, Dai H, Yousaf N, Moussaif M, Deng Y, Boufelliga A, Swamy OR, Leone ME, Riedel H. 1999. Grb10, a positive, stimulatory signaling adapter in platelet-derived growth factor BB-, insulin-like growth factor I-, and insulin-mediated mitogenesis. Mol Cell Biol 19:6217–6228.

Wang L, Balas B, Christ-Roberts CY, Kim RY, Ramos FJ, Kikani CK, Li C, Deng C, Reyna S, Musi N, Dong LQ, DeFronzo RA, Liu F. 2007. Peripheral disruption of the Grb10 gene enhances insulin signaling and sensitivity in vivo. Mol Cell Biol 27:6497–6505.

Wilschut KJ, Jaksani S, Van Den Dolder J, Haagsman HP, Roelen BA. 2008. Isolation and characterization of porcine adult muscle-derived progenitor cells. J Cell Biochem 105:1228–1239.

Yablonka-Reuveni Z, Rivera AJ. 1994. Temporal expression of regulatory and structural muscle proteins during myogenesis of satellite cells on isolated adult rat fibers. Dev Biol 164:588–603.

Yablonka-Reuveni Z, Rivera AJ. 1997. Proliferative Dynamics and the role of FGF2 during myogenesis of rat satellite cells on isolated fibers. Basic Appl Myol 7:189–202.

Yu Y, Yoon SO, Poulogiannis G, Yang Q, Ma XM, Villen J, Kubica N, Hoffman GR, Cantley LC, Gygi SP, Blenis J. 2011. Phosphoproteomic analysis identifies Grb10 as an mTORC1 substrate that negatively regulates insulin signaling. Science 332:1322–1326.